JOURNAL OF GEOPHYSICAL RESEARCH, VOL. 103, NO. D2, PAGES 1799–1805, JANUARY 27, 1998

Incorporation of physical optics effects and computation of the Legendre expansion for ray-tracing phase functions involving δ-function transmission

Michael I. Mishchenko
NASA Goddard Institute for Space Studies, New York

Andreas Macke
Institut für Meereskunde, Kiel, Germany

Abstract. The standard geometric optics (GO) technique predicts that the phase function for large nonspherical particles with parallel plane facets (e.g., hexagonal ice crystals) should have an infinitesimally narrow δ-function transmission peak caused by rays twice transmitted (refracted) in exactly the forward scattering direction. However, exact *T*-matrix computations and physical considerations based on the Kirchhoff approximation suggest that this peak is an artifact of GO completely ignoring physical optics effects and must be convolved with the Fraunhofer pattern, thereby producing a phase function component with an angular profile similar to the standard diffraction component. This convolution can be performed with a simple procedure which supplements the standard ray-tracing code and makes the computation of the phase function and its Legendre expansion both more physically realistic and more accurate.

1. Introduction

It is well known that a convenient way of representing the scattering phase function $P(\Theta)$ for aerosol and cloud particles is expanding it in Legendre polynomials as

$$P(\Theta) = \sum_{n=0}^{n_{\max}} x_n P_n(\cos\Theta), \qquad x_0 \equiv 1, \tag{1}$$

where Θ is the scattering angle, $P_n(\cos\Theta)$ are Legendre polynomials, and the value of the upper summation limit $n_{\max}$ depends on the desired numerical accuracy of the expansion [*van de Hulst*, 1980; *Lenoble*, 1985; *Stephens*, 1994; *Yanovitskij*, 1997]. Since the number of numerically significant terms in the Legendre expansion is finite and often relatively small, this expansion can be used for efficiently computing the phase function for essentially any number of scattering angles with a small consumption of CPU time. Furthermore, the Legendre expansion coefficients x_n can be used to directly compute the Fourier components of the phase function via simple and exact analytical formulas, which is the first step in radiative transfer computations using numerical techniques such as the adding/doubling method [*Hansen and Travis*, 1974; *Wiscombe*, 1976; *van de Hulst*, 1980], the discrete ordinates method [*Stamnes et al.*, 1988; *Nakajima and King*, 1992], and the spherical harmonics method [*Benassi et al.*, 1984].

Copyright 1998 by the American Geophysical Union.

Paper number 97JD03121.
0148-0227/98/97JD-03121$09.00

The Legendre expansion coefficients for the widely used Henyey-Greenstein phase function are given by the simple analytical expression [*van de Hulst*, 1980]

$$x_n = (2n+1)g^n, \tag{2}$$

where g is the asymmetry parameter. Efficient exact methods based on solving Maxwell's equations exist for computing the expansion coefficients for spherical particles [e.g., *de Rooij and van der Stap*, 1984, and references therein], randomly oriented, rotationally symmetric nonspherical particles [*Mishchenko*, 1991], and randomly oriented clusters of spheres [*Mackowski and Mishchenko*, 1996]. For irregular particles with sizes much larger than the wavelength of the incident radiation, such as cirrus cloud particles in the visible, direct numerical solutions of Maxwell's equations do not currently exist. Therefore the expansion coefficients have to be computed by using an approximate technique such as the geometric optics (GO) approximation. Using the orthogonality property of Legendre polynomials, we easily derive from equation (1)

$$x_n = \frac{2n+1}{2} \int_0^{\pi} d\Theta\, P(\Theta) P_n(\cos\Theta) \sin\Theta. \tag{3}$$

The integral in equation (3) can be calculated numerically by using a quadrature formula provided that the phase function values at the quadrature division points are known. This numerical approach works well if the phase function is rather smooth but becomes problematic for particles having parallel planes such as hexagonal columns and plates, cubes, or finite circular cylinders. In this case, the standard GO predicts a

strong, infinitesimally narrow peak in the exact forward scattering direction which is caused by rays that undergo two refractions through parallel plane facets and is superimposed on the diffraction component of the phase function. This effect was called by *Takano and Liou* [1989] the δ-function transmission.

It is obvious, however, that GO predicts the infinitesimally narrow δ-function transmission peak only because it completely ignores physical optics effects. Simple physical optics considerations similar to those of *Muinonen* [1989] and *Muinonen et al.* [1989] cause us to conclude that although a strong nondiffraction forward scattering peak does exist and can be qualitatively explained in GO terms as a manifestation of the δ-function transmission, it nonetheless has an appreciable angular width comparable to that of the Fraunhofer diffraction peak and a diffraction-like angular profile. In the following sections we use exact *T*-matrix computations to substantiate this conclusion and describe a simple modification of the standard ray-tracing procedure which makes GO computations more physically realistic and accurate. Furthermore, we show that this modified procedure significantly simplifies and makes more accurate the numerical computation of the Legendre expansion coefficients for particles with parallel plane facets.

2. Definitions

The ray-tracing technique assumes the representation of an incident plane electromagnetic wave as a sufficiently large number of incoherent parallel rays. Each individual ray is independently traced for a given particle geometry and orientation using Snell's law and Fresnel's equations [*Jackson*, 1975]. All escaping rays are sampled into incremental solid angle elements (bins) centered at predefined discrete scattering angles from 0° to 180°. This procedure yields the angular distribution of the scattered intensity and is repeated for a sufficiently large number of particle orientations with respect to the incident beam in order to simulate the three-dimensional (3-D) random orientation. The geometric optics scattering phase function $P_{GO}(\Theta)$ is finally given by

$$\frac{1}{4\pi} P_{GO}(\Theta_i)\,\Delta\Omega_i = \frac{E_i}{\sum_{i=1}^{M} E_i}, \tag{4}$$

where Θ_i (i = 1, 2, ..., M) are discrete scattering angles covering the entire interval [0°, 180°], $\Delta\Omega_i = 2\pi \sin\Theta_i\, \Delta\Theta_i$ are the corresponding incremental solid angle elements such that

$$\sum_{i=1}^{M} \Delta\Omega_i = 4\pi, \tag{5}$$

and E_i is the energy accumulated in the ith solid angle element. Thus $P_{GO}(\Theta)$ satisfies the normalization condition

$$\frac{1}{4\pi} \int_{4\pi} d\Omega\, P_{GO}(\Theta) = 1, \tag{6}$$

and $(1/4\pi)P_{GO}(\Theta)d\Omega$ describes the probability for an incident ray to be scattered into the solid angle element $d\Omega$ centered at the scattering angle Θ. The final step in computing the full scattering phase function is supplementing the ray-tracing computation by the computation of the Fraunhofer diffraction component which significantly deviates from zero only in the vicinity of the forward scattering direction [*van de Hulst*, 1957]. We thus have

$$P(\Theta) = \frac{w_{GO} P_{GO}(\Theta) + P_D(\Theta)}{w_{GO} + 1}, \tag{7}$$

where w_{GO} is the geometric optics single-scattering albedo, and $P_D(\Theta)$ is the diffraction phase function. Assuming for simplicity the circular particle projection, we have for the diffraction phase function in the limit $x \to \infty$ [*van de Hulst*, 1957]

$$\begin{cases} P_D(\Theta) = 4x^2 \left[\dfrac{J_1(x\sin\Theta)}{x\sin\Theta}\right]^2, & \Theta \in [0°, 90°], \\ P_D(\Theta) = 0, & \Theta \in [90°, 180°]. \end{cases} \tag{8}$$

In equation (8), $J_1(y)$ is the Bessel function of the first kind, and x is the size parameter. Note that the truncation of the diffraction phase function in equation (8) at Θ = 90° can induce a step function like singularity in the phase function for smaller size parameter particles. The magnitude of this singularity can be used as an additional criterion in determining the smallest size parameter to which the ray-tracing approximation can be applied. For large x,

$$\frac{1}{4\pi} \int_{4\pi} d\Omega\, P_D(\Theta) = 1 - \frac{J_1(2x)}{x} = 1 + O\left(x^{-3/2}\right), \tag{9}$$

so that the diffraction phase function is asymptotically normalized to unity.

We have from equation (4)

$$P_{GO}(\Theta_i) = 4\pi \lim_{\Delta\Omega_i \to 0} \frac{E_i}{\Delta\Omega_i \sum_{j=1}^{M} E_j}, \tag{10}$$

which means that a numerically accurate computation of the GO phase function at a scattering angle Θ_i may, in principle, require choosing a rather small solid angle element $\Delta\Omega_i$ and thus tracing a large number of rays and averaging over many orientations. Quite often P_{GO} is a rather smooth function of the scattering angle, and the numerical evaluation of the limit of equation (10) encounters no difficulties because its right-hand side converges at a relatively large $\Delta\Theta_i$. For example, *Macke et al.* [1996] have found that in most cases it is sufficient to use solid angle bins with Δ Θ = 1°, trace 300 rays for each particle orientation, and average over 30,000 orientations. However, for crystals with parallel plane facets the right-hand side of equation (10) does not converge to a finite limit at Θ = 0. This is a manifestation of what *Takano and Liou* [1989] call the δ-function transmission.

3. *T*-Matrix Computations

As mentioned in the introduction, the δ-function transmission is not a real phenomenon but is rather an

artifact of GO completely ignoring physical optics effects. *Muinonen et al.* [1989] used the Kirchhoff approximation [*Jackson*, 1985; *Muinonen*, 1989; *Arnott and Marston*, 1991] to show that a plane wave front emerging from a crystal face should spread and produce a Fraunhofer-type pattern in the radiation zone. The corrected size-dependent phase function is thus obtained through a convolution of the GO phase function and the Fraunhofer pattern. *Muinonen et al.* [1989] used this physical optics correction to modify the true and corner retroreflection peaks computed originally from geometric optics for large parallelepipeds and hexagonal crystals. It is clear that the same physical optics correction must also be applied to the δ-function transmission.

Recently, *Mishchenko et al.* [1997] have used the improved version of the exact *T*-matrix method [*Waterman*, 1971; *Mishchenko et al.*, 1996a, b; *Wielaard et al.*, 1997] to compute the scattering of light by large nonspherical ice particles. Computations for circular disks with size parameters up to 50 and aspect ratios up to 3 have shown that the physical optics correction based on the Kirchhoff approximation produces excellent results when applied to light externally reflected by large plane facets of ice crystals. In this paper, we perform similar *T*-matrix computations in order to verify the applicability of the physical optics correction to the δ-function transmission component of the phase function. Specifically, we compute the exact phase function for a monodisperse oblate spheroid with the aspect ratio 3 and size parameter $x = 2\pi a/\lambda = 50$, where a is the spheroid major semiaxis and λ is the wavelength of the incident light, and a circular disk with the diameter-to-height ratio 3 and the same size parameter $x = 2\pi r/\lambda = 50$, where r is the disk radius. The refractive index is $1.3082 + i0.1328 \times 10^{-7}$ and is typical of water ice at visible wavelengths [*Warren*, 1984]. Although the size parameter 50 does not necessarily put the particles in the geometric optics domain [*Macke et al.*, 1995; *Wielaard et al.*, 1997], it nonetheless is big enough to make relevant an interpretation of the exact *T*-matrix computations in terms of the geometric optics and Kirchhoff approximations.

We assume that the external light is unpolarized and is incident along the rotational axes of the particles so that both particles have exactly the same circular projections perpendicular to the incident light and thus exactly the same diffraction contributions to the total phase function. The *T*-matrix computations show that the phase function value at $\Theta = 0$ for the circular disk is greater than that for the spheroid by as large a factor as 2.7. However, despite the large difference in the amplitudes of the forward scattering peaks for the two phase functions, their angular profiles, defined as $P(\Theta)/P(0°)$, are almost the same (Figure 1), so the half widths at half maximum of the two peaks differ by only 10%.

These results can be explained as follows: The circular disk gives two strong contributions to the phase function at zero scattering angle, one due to diffraction and another due to rays twice refracted in the forward direction by the large parallel plane facets. Because of the optical physics effect [*Muinonen et al.*, 1989] the angular profiles of both contributions are similar. On the other hand, the spheroid produces only the strong diffraction component. As a result, the total phase function value at $\Theta = 0°$ for the disk is much greater, whereas the angular profiles of the phase functions for the disk and the spheroid are nearly the same. This explanation shows that the angular profile of the δ-function transmission peak for the disk is not a true δ function but is rather described by the same Fraunhofer pattern as the standard diffraction peak. Importantly, diffraction contributes 71% of the total phase function value at $\Theta = 0$ for the spheroid and only 26% for the disk, thus demonstrating that the δ-function transmission can be the dominant contributor to the forward scattering phase function for transparent particles with large parallel planes.

To verify this interpretation of the *T*-matrix calculations, we have computed the scattering of light by the same particles and with the same real part of the refractive index, but with a much larger imaginary part equal to 0.1. Figure 2 shows that the angular profiles of the phase functions for the strongly absorbing particles in the vicinity of the forward scattering direction are essentially the same. Even the secondary intensity maxima at about 5.5° almost coincide. Also, the ratio of the forward scattering phase function values for the disk and the spheroid is now only 1.23. These results can be easily explained by the effect of absorption which strongly suppresses the δ-function transmission contribution for the disk and makes diffraction the dominant contributor to the forward scattering part of both phase functions. Indeed, diffraction now contributes more than 93% of the total phase function value at $\Theta = 0°$ for the spheroid and more than 75% for the disk.

Comparison of Figures 1 and 2 shows that the two solid curves computed for the nonabsorbing and strongly absorbing disks, respectively, are almost identical. In fact, plotting the

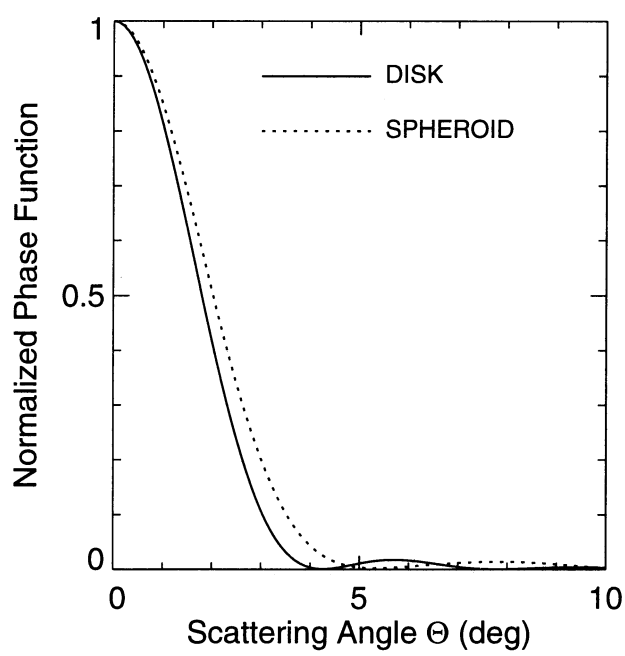

Figure 1. Normalized phase function $P(\Theta)/P(0°)$ versus scattering angle for a circular disk with the diameter-to-height ratio 3 and size parameter $x = 2\pi r/\lambda = 50$, where r is the disk radius, and an oblate spheroid with the aspect ratio 3 and the same size parameter $x = 2\pi a/\lambda = 50$, where a is the spheroid major semiaxis. The external unpolarized light is incident along the rotational axes of the particles. The refractive index is $1.3082 + i0.1328 \times 10^{-7}$.

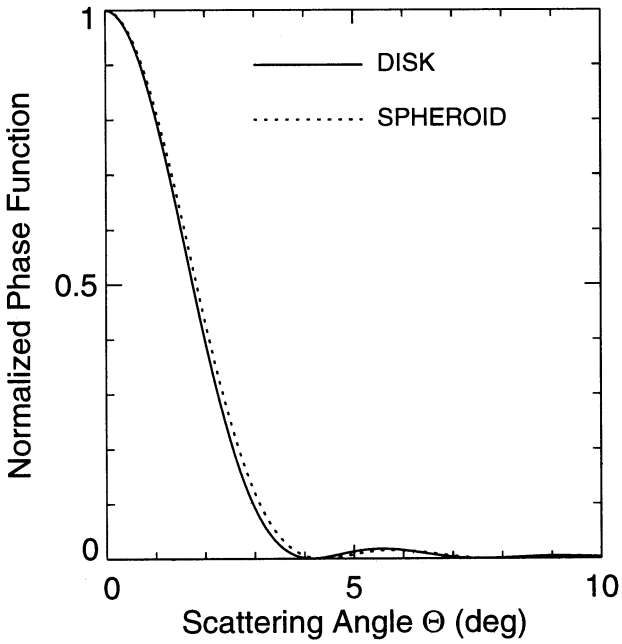

Figure 2. As in Figure 1 but for the refractive index 1.3082 + i0.1.

curves in the same diagram makes them hardly distinguishable (Figure 3). In view of the quite different relative contributions of the diffraction and δ-function transmission components in these two cases, Figure 3 unequivocally demonstrates that the angular profiles of the diffraction and δ-function transmission peaks for a disk are indeed the same. Also, increasing absorption has brought the dotted curve in Figure 2 to a closer agreement with the respective curve for the disk than in Figure 1. This suggests that the small discrepancies between the solid and dotted curves in Figure 1 are caused by the ray tracing component of the forward-scattering phase function for the transparent spheroid which is not fully described by the Fraunhofer angular profile.

The final check is provided by computing the scattering of an obliquely incident beam. In this case the scattering problem is not rotationally symmetric, and the existence of a δ-function transmission component with the same angular profile as the diffraction component could not be misinterpreted as specific to axially symmetric configurations only. Figure 4 is computed for the same nonabsorbing ice particles as Figure 1, but now the incident light is directed at an angle of 20° with the particle axis. The scattering plane is the plane through the particle axis and the incident beam, and the normalized phase function is plotted versus the angle between the particle axis and the scattered beam. Both particles produce strong intensity peaks centered at exactly the forward scattering direction and having essentially the same angular profiles. However, the forward scattering phase function value for the disk is greater than that for the spheroid by a factor of 1.9. This large factor can only be explained by a strong δ-function transmission contribution for the disk. This contribution is smaller than in the symmetric case because fewer incident rays can now be transmitted in the exact forward scattering direction and also

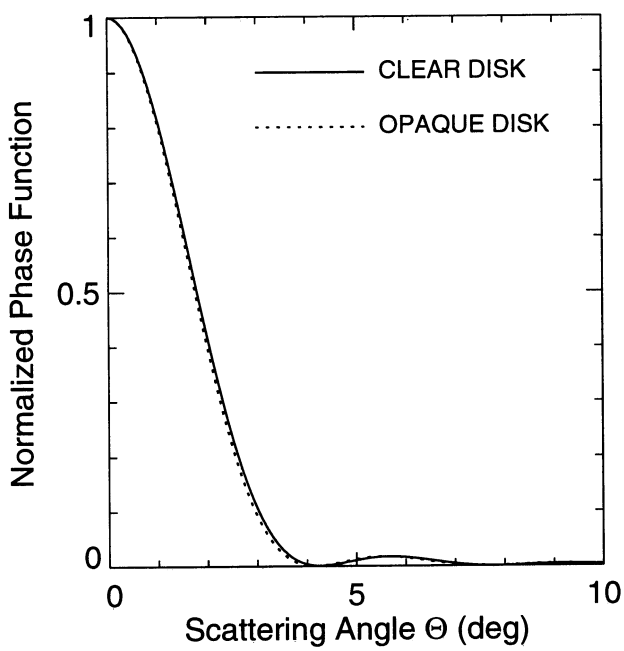

Figure 3. Normalized phase function $P(\Theta)/P(0°)$ versus scattering angle for circular disks with the diameter-to-height ratio 3 and size parameter $x = 2\pi r/\lambda = 50$. The refractive indices are $1.3082 + i0.1328 \times 10^{-7}$ (solid curve) and 1.3082 + i0.1 (dotted curve). The external unpolarized light is incident along the rotational axes of the particles.

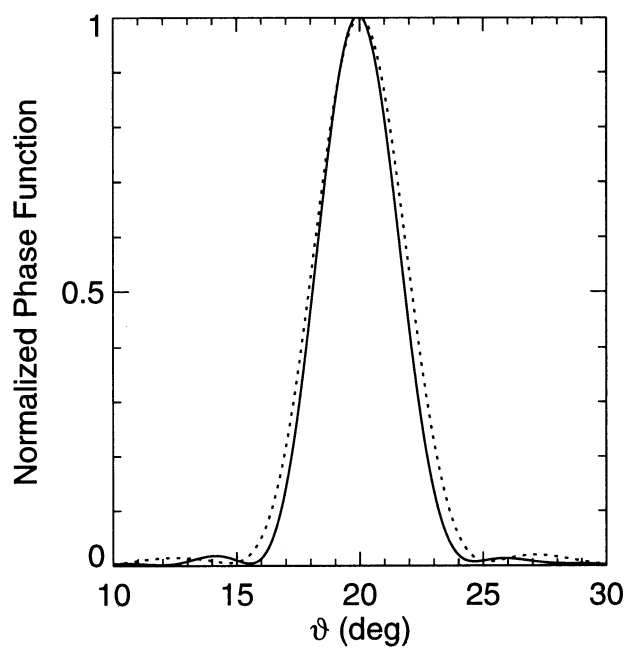

Figure 4. Normalized phase function $P(\vartheta)/P(20°)$ versus the angle between the particle axis and the scattered beam, ϑ, for a circular disk with the diameter-to-height ratio 3 and size parameter $x = 2\pi r/\lambda = 50$ (solid curve) and an oblate spheroid with the aspect ratio 3 and the same size parameter $x = 2\pi a/\lambda = 50$ (dotted curve). The angle between the particle axis and the unpolarized incident beam is 20°. The scattering plane is the plane through the particle axis and the incident beam. The refractive index is $1.3082 + i0.1328 \times 10^{-7}$.

because of an increased contribution of the side surface of the disk to the forward scattered light. However, the δ-function transmission component still dominates the total phase function value at the exact forward scattering direction and has the same angular profile as the diffraction component.

4. Modified Ray-Tracing Procedure

Thus the exact T-matrix computations show that the GO phase function for crystals with parallel plane facets must indeed be corrected by convolving the GO δ-function transmission peak with the Fraunhofer angular pattern. This convolution can be accomplished with the following simple procedure. The ray-tracing code described by *Macke et al.* [1996] uses 181 solid angle bins centered at scattering angles $\Theta_i = 0.25°, 1°, 2°, ..., 178°, 179°$ and $179.75°$. For the first and the last bins, $\Delta\Theta_1 = \Delta\Theta_{181} = 0.5°$, while for all other bins, $\Delta\Theta_i = 1°$. By definition the ray-tracing phase function satisfies the normalization condition

$$\frac{1}{4\pi}\sum_{i=1}^{181} P_{\mathrm{GO}}(\Theta_i)\Delta\Omega_i = 1. \tag{11}$$

All energy resulting from the δ-function transmission is accumulated in the first bin, thereby causing $P_{\mathrm{GO}}(\Theta_1) \gg P_{\mathrm{GO}}(\Theta_i)$, $i = 2, ..., 181$. Since our goal is to replace the artificial δ-function transmission peak with a diffraction-like component, we need to know the amount of energy contained in the peak. Therefore we replace the large $P_{\mathrm{GO}}(\Theta_1)$ value with the much smaller $P_{\mathrm{GO}}(\Theta_2)$ value and denote the truncated ray-tracing phase function by P'_{GO}. This modified phase function is a rather slowly varying function of the scattering angle, so phase function values at scattering angles not coinciding with Θ_i can be accurately computed by using linear interpolation/extrapolation. We then compute the quantity

$$\delta = 1 - \frac{1}{4\pi}\sum_{i=1}^{181} P'_{\mathrm{GO}}(\Theta_i)\Delta\Omega_i, \tag{12}$$

which determines the fractional contribution of the diffraction-like forward scattering component to the ray-tracing phase function. The new ray-tracing phase function is thus given by

$$P_{\mathrm{GO}}(\Theta) = P'_{\mathrm{GO}}(\Theta) + \delta P_{\mathrm{D}}(\Theta), \tag{13}$$

where $P_{\mathrm{D}}(\Theta)$ is given by equation (8). Inserting equation (13) into equation (7), we finally derive the total phase function as

$$P(\Theta) = \frac{w_{\mathrm{GO}}P'_{\mathrm{GO}}(\Theta) + (1 + w_{\mathrm{GO}}\delta)P_{\mathrm{D}}(\Theta)}{w_{\mathrm{GO}} + 1}. \tag{14}$$

The corresponding total single-scattering albedo is given by

$$w = \frac{w_{\mathrm{GO}} + 1}{2}. \tag{15}$$

It is easy to verify that the phase function of equation (14) is normalized such that

$$\frac{1}{4\pi}\int_{4\pi} d\Omega\, P(\Theta) = 1. \tag{16}$$

Rewriting equation (3) as

$$x_n = \frac{2n+1}{2}\int_{-1}^{1} d\mu\, P(\mu)P_n(\mu), \qquad \mu = \cos\Theta \tag{17}$$

and using a Gaussian quadrature formula on the interval [−1, 1], we have

$$x_n = \frac{2n+1}{2}\sum_{j=1}^{N_{\mathrm{G}}} P(\mu_j)P_n(\mu_j)w_j, \tag{18}$$

where μ_j and w_j ($j = 1, ..., N_{\mathrm{G}}$) are Gaussian division points and weights, respectively. Since the diffraction phase function P_{D} is given by an exact analytical expression and the modified ray-tracing phase function P'_{GO} is a slowly varying function of the scattering angle and can be accurately interpolated/extrapolated, the total phase function values at the division points can be computed rather precisely. As a result, the numerical evaluation of equation (18) encounters no difficulties and produces accurate values of the Legendre expansion coefficients. The accuracy of computing the expansion coefficients can be checked by evaluating the right-hand side of equation (1) at the Gaussian division points and comparing the result with the original phase function values. Such checks have shown that the accuracy of the Legendre representation of the phase function can be made arbitrarily high by including a sufficiently large number $n_{\max}$ of the expansion coefficients. We have found that a reliable criterion for choosing an adequate value of $n_{\max}$ is checking that the right-hand side of equation (1) computed for $\Theta = 0$ exactly coincides with the forward scattering value of the original phase function.

As an example, in Figure 5 we show the total phase function for polydisperse, randomly oriented hexagonal columns with length-to-diameter ratio 2 and distribution of surface-equivalent sphere radii given by the standard power law [*Hansen and Travis*, 1974]:

$$n(r) = \begin{cases} \dfrac{2r_1^2 r_2^2}{r_2^2 - r_1^2}\, r^{-3} & r_1 \le r \le r_2, \\ 0 & \text{otherwise}. \end{cases} \tag{19}$$

The parameters r_1 and r_2 are chosen such that the effective radius and effective variance of the distribution, as defined by *Hansen and Travis* [1974], are $r_{\mathrm{eff}} = 40$ μm and $v_{\mathrm{eff}} = 0.2$. The refractive index is $1.3082 + i0.1328\times10^{-7}$, and the wavelength is $\lambda = 0.645$ μm. The solid curve shows the original phase function, while the dotted curve shows the result of evaluating the Legendre expansion of equation (1) with $n_{\max} = 1000$ terms. It is seen that the original phase function and the Legendre expansion almost perfectly coincide (relative differences less than 10^{-5}). The forward scattering value for this phase function is 1.160×10^5 and the asymmetry parameter is 0.8209.

5. Discussion and Conclusions

It is clear that however large a particle is compared to the wavelength, physical optics effects will preclude the

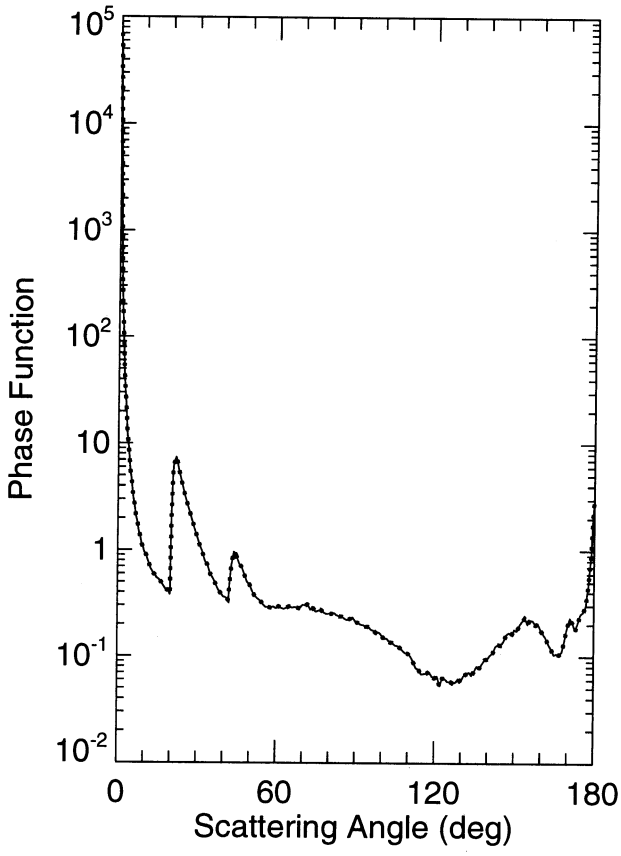

Figure 5. Scattering phase function for polydisperse, randomly oriented hexagonal ice columns with length-to-diameter ratio 2. The solid curve shows the original phase function and the dotted curve shows the result of evaluating the Legendre expansion of equation (1) with 1000 terms.

appearance of perfect singularities in the scattering pattern like the δ-function transmission peak in the phase function. Instead, as *Muinonen et al.* [1989] have pointed out, a wave front emerging from a flat crystal facet should spread and produce an angular intensity distribution in the far-field zone similar to the well-known Fraunhofer diffraction pattern. In the theoretical limit of an infinite size parameter the δ-function transmission peak becomes a true δ function. However, the angular width of the δ-function transmission peak is always comparable to that of the Kirchhoff diffraction component, and as long as the latter is computed explicitly by using formulas analogous to equation (8), so should be the δ-function transmission component.

In this paper, we first used exact *T*-matrix computations for rather large nonspherical particles to demonstrate that the effect that can be interpreted in geometric optics terms as δ-function transmission through parallel planes indeed results in a quasi-Fraunhofer forward scattering peak rather than in a true δ-function peak. We then described a very simple numerical procedure which incorporates this physical optics effect in the standard ray-tracing computation of the phase function for large particles with parallel plane facets. This procedure not only makes ray-tracing computations more physically relevant but also simplifies and makes more accurate the computation of the phase function and its Legendre expansion. It should be noted that our specific procedure may not be the only practical way of incorporating the δ-function transmission component using the physical optics approximation [cf. *Yang and Liou*, 1996]. Also, its accuracy for very large particles cannot be assessed directly due to the lack of exact theoretical methods based on solving Maxwell's equations and applicable to size parameters exceeding a few hundred. However, our approach is physically based and appears to be very simple and well justified since it consists of directly computing the amount of energy contained in the δ-function transmission peak and convolving it with the Fraunhofer angular pattern.

As one of the reviewers of this paper has characterized our procedure, it is yet another patch for the ray-tracing approach to scattering problems. The ray-tracing technique has many disadvantages like the ignorance of the crossing of caustics or the interference of waves and dealing immediately with irradiance rather than with electric fields. These factors can degrade significantly the accuracy of ray-tracing computations, often in an unpredictable way. However, the lack of exact methods applicable to large ice crystals may make patches like this one useful, at least for the near future.

In addition to the δ-function transmission component the phase function shown in Figure 5 exhibits a pronounced corner retroreflection peak centered at $\Theta = 180°$ and having an infinitesimal angular width in the framework of the standard ray-tracing approximation. As suggested by *Muinonen et al.* [1989], this peak should also be convolved with the Fraunhofer angular pattern, and this can be done in a way similar to that described in the previous section. However, the amount of energy concentrated in the corner retroreflection peak is small as compared to that of the δ-function transmission peak, thus making the latter correction less important.

Acknowledgments. We thank two anonymous reviewers for valuable comments and suggestions and N. T. Zakharova for help with graphics. This work was supported by the NASA FIRE III program and grant No. N00014-96-1-G020 from the Naval Research Laboratory.

References

Arnott, W. P., and P. L. Marston, Unfolded optical glory of spheroids: backscattering of laser light from freely rising spheroidal air bubbles in water, *Appl. Opt.*, *30*, 3429-3442, 1991.

Benassi, M., R. D. M. Garcia, A. H. Karp, and C. E. Siewert, A high-order spherical harmonics solution to the standard problem in radiative transfer, *Astrophys. J.*, *280*, 853-864, 1984.

de Rooij, W. A., and C. C. A. H. van der Stap, Expansion of Mie scattering matrices in generalized spherical functions, *Astron. Astrophys.*, *131*, 237-248, 1984.

Hansen, J. E., and L. D. Travis, Light scattering in planetary atmospheres, *Space Sci. Rev.*, *16*, 527-610, 1974.

Jackson, J. D., *Classical Electrodynamics*, John Wiley, New York, 1975.

Lenoble, J. (ed.), *Radiative Transfer in Scattering and Absorbing Atmospheres: Standard Computational Procedures*, 300 pp., A. Deepak, Hampton, Va., 1985.

Macke, A., M. I. Mishchenko, K. Muinonen, and B. E. Carlson, Scattering of light by large nonspherical particles: ray-tracing approximation versus *T*-matrix method, *Opt. Lett.*, *20*, 1934-1936, 1995.

Macke, A., J. Mueller, and E. Raschke, Single scattering properties of atmospheric ice crystals, *J. Atmos. Sci.*, *53*, 2813-2825, 1996.

Mackowski, D. W., and M. I. Mishchenko, Calculation of the *T* matrix and the scattering matrix for ensembles of spheres, *J. Opt. Soc. Am. A*, *13*, 2266-2278, 1996.

Mishchenko, M. I., Light scattering by randomly oriented axially symmetric particles, *J. Opt. Soc. Am. A*, *8*, 871-882, 1991.

Mishchenko, M. I., L. D. Travis, and D. W. Mackowski, *T*-matrix computations of light scattering by nonspherical particles: A review, *J. Quant. Spectrosc. Radiat. Transfer*, *55*, 535-575, 1996a.

Mishchenko, M. I., L. D. Travis, and A. Macke, Scattering of light by polydisperse, randomly oriented, finite circular cylinders, *Appl. Opt.*, *35*, 4927-4940, 1996b.

Mishchenko, M. I., D. J. Wielaard, and B. E. Carlson, *T*-matrix computations of zenith-enhanced lidar backscatter from horizontally oriented ice plates, *Geophys. Res. Lett.*, *24*, 771-774, 1997.

Muinonen, K., Scattering of light by crystals: A modified Kirchhoff approximation, *Appl. Opt.*, *28*, 3044-3050, 1989.

Muinonen, K., K. Lumme, J. Peltoniemi, and W. M. Irvine, Light scattering by randomly oriented crystals, *Appl. Opt.*, *28*, 3051-3060, 1989.

Nakajima, T., and M. D. King, Asymptotic theory for optically thick layers: Application to the discrete ordinates method, *Appl. Opt.*, *31*, 7669-7683, 1992.

Stamnes, K., S.-C. Tsay, W. Wiscombe, and K. Jayaweera, Numerically stable algorithm for discrete-ordinate-method radiative transfer in multiple scattering and emitting layered media, *Appl. Opt.*, *27*, 2502-2509, 1988.

Stephens, G. L., *Remote Sensing of the Lower Atmosphere*, 523 pp., Oxford Univ. Press, New York, 1994.

Takano, Y., and K.-N. Liou, Solar radiative transfer in cirrus clouds, 1, Single-scattering and optical properties of hexagonal ice crystals, *J. Atmos. Sci.*, *46*, 3-19, 1989.

van de Hulst, H. C., *Light Scattering by Small Particles*, 470 pp., John Wiley, New York, 1957.

van de Hulst, H. C., *Multiple Light Scattering*, 739 pp., Academic, San Diego, Calif., 1980.

Warren, S. G., Optical constants of ice from the ultraviolet to the microwave, *Appl. Opt.*, *23*, 1206-1225, 1984.

Waterman, P. C., Symmetry, unitarity, and geometry in electromagnetic scattering, *Phys. Rev. D Part. Fields*, *3*, 825-839, 1971.

Wielaard, D. J., M. I. Mishchenko, A. Macke, and B. E. Carlson, Improved *T*-matrix computations for large, nonabsorbing and weakly absorbing nonspherical particles and comparison with geometric optics approximation, *Appl. Opt.*, *36*, 4305-4313, 1997.

Wiscombe, W. J., On initialization, error and flux conservation in the doubling method, *J. Quant. Spectrosc. Radiat. Transfer*, *16*, 637-658, 1976.

Yang, P., and K. N. Liou, Geometric-optics–integral-equation method for light scattering by nonspherical ice crystals, *Appl. Opt.*, *35*, 6568-6584, 1996.

Yanovitskij, E. G., *Light Scattering in Inhomogeneous Atmospheres*, 371 pp., Springer-Verlag, New York, 1997.

A. Macke, Institut für Meereskunde, Abt. Maritime Meteorologie, Duesternbrooker Weg 20, 24105 Kiel, Germany. (e-mail: amacke@ifm.uni-kiel.de)

M. I. Mishchenko, NASA Goddard Institute for Space Studies, 2880 Broadway, New York, NY 10025. (e-mail: crmim@giss.nasa.gov)

(Received March 19, 1997: revised August 12, 1997; accepted October 23, 1997.)